Fast simulation of stochastic exposure distribution in electron-beam lithography

Xinyu Zhao and Soo-Young Lee[a)]
Department of Electrical and Computer Engineering, Auburn University, Auburn, Alabama 36849

Sang-Hee Lee, Byung-Gook Kim, and Han-Ku Cho
Photomask Division, Samsung Electronics, 16 Banwol-Dong, Hwasung 445-701, Kyunggi-Do, Korea

(Received 30 June 2012; accepted 30 October 2012; published 26 November 2012)

The relative critical dimension variation of nanoscale features has become large enough to significantly affect the minimum feature size and maximum circuit density realizable in most lithographic processes. One source of such variation is the line edge roughness (LER). In the electron-beam lithographic process, the fluctuation of exposure (energy deposited) in the resist is one of the main factors contributing to the LER. It is essential to accurately estimate the exposure fluctuation for developing an effective method to reduce the LER. A possible method is to rely on the Monte Carlo simulation in computing the exposure distribution in a circuit pattern, i.e., generating a point spread function (PSF) for each point to be exposed, where the PSF is stochastic. While this approach can lead to a more realistic estimation, it is not practical due to its tremendous amount of computation required. In this paper, a new method to greatly reduce the number of PSF's to be generated without sacrificing the accuracy of estimating the exposure fluctuation is described. It generates only a small number of stochastic PSF's and uses them randomly in the exposure calculation for a circuit pattern. Through an extensive simulation, it is shown that the new method is statistically equivalent to generating a PSF for each point with an acceptable error. Since it is not necessary to know the exact spatial distribution of exposure for estimation of the LER, the new method has a good potential to be employed in practice to reduce the computation time by orders of magnitude. © *2012 American Vacuum Society*. [http://dx.doi.org/10.1116/1.4767447]

I. INTRODUCTION

Electron-beam (e-beam) lithography is widely employed in transferring circuit patterns onto resist, including three-dimensional structures.[1–4] Its main drawbacks are the low throughput due to pixel-by-pixel or feature-by-feature writing and the proximity effect caused by electron scattering. Nevertheless, its capability of writing ultrafine features still finds a variety of applications, such as fabrication of photomasks, imprint lithography molds, experimental circuit patterns, etc. Correction of the proximity effect has been investigated over three decades by several researchers in an effort to minimize the CD (critical dimension) error and eventually increase the circuit density.[5–7] Another related issue is the variation of CD within a pattern or among patterns due to the stochastic nature of lithographic and developing processes. Note that the CD variation is a common problem of all types of lithography. The relative CD variation compared to the feature size has become significant as the minimum feature size goes well below 100 nm and can significantly affect the minimum feature size and maximum circuit density realizable in practice.[8] A quantitative measure of such variation which is being extensively studied these days is the line edge roughness (LER).[9] The studies include modeling, estimation, and reduction of LER. The objective of our recent research project is to develop an effective way to minimize the LER for the e-beam lithographic process. As a first step, an efficient way to estimate the LER is being investigated.

In e-beam lithography, one of the main sources of the LER is the fluctuation or stochastic distribution of exposure (energy deposited) in the resist, which leads to the variation of CD after development. In several studies,[10–12] an analytic model such as Anderson model was formulated to estimate the LER. However, accuracy of the parameters required in such a model is not guaranteed. The focus of this paper is on designing a method for simulating the exposure fluctuation throughout the resist fast and accurately. In order to simulate the stochastic exposure distribution in the resist, one may employ the Monte Carlo simulation.[13–16] A possible method, to be referred to as *direct* Monte Carlo method (DMC), is to generate a separate (instance of) point spread function (PSF), for each exposed point in a circuit pattern, which describes the exposure distribution in the resist when a point is exposed. While the exposure distribution derived (through convolution) by this method can be realistic, it is not practical since the number of points (or PSF's to be generated) is tremendous and generating a PSF requires a long computation time.[17] A new method proposed in this paper reduces the number of PSF's greatly without sacrificing the accuracy of estimating the exposure fluctuation substantially.

The key idea of the new method is to generate a small number of (stochastic) PSF's and use them randomly in the exposure calculation for a circuit pattern, to be referred to as *simplified* Monte Carlo method (SMC). For each point exposed, a PSF is selected randomly from the set of PSF's generated. Since the number of PSF's generated is much smaller than the number of points exposed, the computation required would not be overwhelming. The validity of the

[a)]Electronic mail: leesooy@eng.auburn.edu

Downloaded 10 Dec 2012 to 131.204.21.179. Redistribution subject to AVS license or copyright; see http://avspublications.org/jvstb/about/rights_and_permissions

method has been verified through extensive simulation with two measures of exposure fluctuation, i.e., standard deviation (SD) and power spectral density (PSD).

The rest of the paper is organized as follows. The general model of LER simulation is described in Sec. II. The model and method of *direct* Monte Carlo are briefly reviewed in Sec. III. The *simplified* Monte Carlo method will be introduced in Sec. IV. The simulation procedures are described in Sec. V. Results are discussed in Sec. VI. A summary is provided in Sec. VII.

II. SIMULATION OF LER

In e-beam lithography, the LER is mainly due to the stochastic nature of e-beam exposing and resist developing processes. The electron scattering in the resist is a stochastic process and therefore the exposure distribution for a point exposed, i.e., a PSF, is stochastic. Even when a constant dose is given to a long line, the exposure along the edge of the line fluctuates leading to the edge roughness. The resist developing process also involves a significant level of randomness, which contributes to the LER. Especially in the case of chemically amplified resist, the photoacid generator tends to increase the LER, depending on its density and distribution. Modeling the LER is an important step toward developing a method to minimize it.

One of the approaches to modeling the LER, which can lead to realistic results, is to employ the Monte Carlo simulation[18–20] in obtaining the stochastic distribution of exposure in the resist layer. Then, the LER is estimated from the remaining resist profile derived through the simulation of developing process. However, in this study, the focus is placed on simulating the stochastic fluctuation of exposure in the resist through the Monte Carlo simulation, without the simulation of resist development, due to the following reasons. First, a significant portion of LER comes from the stochastic distribution (or fluctuation) of exposure and therefore consideration of the exposure distribution only is sufficient. Second, the computation of exposure distribution is independent of the estimation of resist profile and is complete by itself. Third, the estimated resist profile heavily depends on the developing process assumed and the development simulation method employed. Therefore, inclusion of the resist development simulation may skew results from analyzing the proposed method.

A fundamental limitation of employing the Monte Carlo simulation is that it requires the tremendous amount of computation due to a large number of pixels in a circuit pattern for each of which a PSF (an instance of stochastic PSF) needs to be generated. Therefore, a method which is fast and accurate (statistically equivalent) in simulating the stochastic exposure distribution would be a useful tool for the LER research.

III. DIRECT MONTE CARLO METHOD

The most realistic way to simulate the stochastic exposure distribution in the resist is to employ the Monte Carlo simulation at each point exposed by the e-beam. Individual electrons incident at each point to be exposed are traced through scattering and energy-deposition processes. This is equivalent to generating an instance of stochastic PSF (to be referred to as a PSF hereafter) for each point. Let N_c denote the number of points to be exposed in a circuit pattern. The set of PSF's generated may be represented by $S = \{psf_i(x,y,z) | i = 1, \cdots, N_c\}$ where i is the PSF index or the index for points exposed. In this study, it is assumed as usual that the process of exposing a pattern by e-beam can be modeled by a linear system. Accordingly, the 3D exposure distribution $e(x, y, z)$ in the resist is computed by the convolution between the PSF and the dose distribution function $d(x, y, 0)$ defined at the surface of resist (see Fig. 1),

$$e(x,y,z) = \int\int d(x-x', y-y', 0) psf_i(x', y', z)\, \mathrm{d}x'\mathrm{d}y', \quad (1)$$

where

$$d(x,y,0) = \begin{cases} D & \text{for exposed points} \\ 0 & \text{otherwise.} \end{cases} \quad (2)$$

Note that Eq. (1) is a *spatially varying* convolution since the PSF varies spatially, i.e., $psf_i(x,y,z)$ from the set S is used for the ith point exposed. In the remainder of the paper, the term "convolution" refers to the spatially varying convolution.

The fundamental limitation of this approach (to be referred to as DMC method) is that its computational complexity is too high to be practical for most patterns of realistic size. Let N_d denote the number of electrons incident at each point for a given dose D, i.e., $N_d = \frac{Dp^2}{q}$ where p is the distance between two adjacent points and q is the charge of electron. Then, the total number of electrons, N_e, to be traced in the simulation is $N_d N_c$. Note that N_c is usually very large.

IV. SIMPLIFIED MONTE CARLO METHOD

As mentioned above, the DMC method is too time-consuming to be employed for a realistic size of circuit pattern. Hence, a new method which is more computationally feasible is needed. Since PSF's are stochastic and only certain measures of exposure fluctuation, not the exposure distribution itself, are of interest, N_c PSF's do not need to be

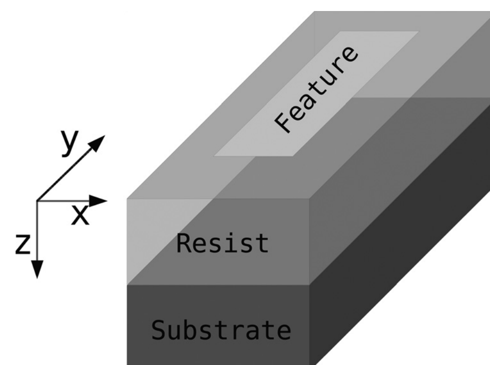

FIG. 1. 3D model of substrate system.

Downloaded 10 Dec 2012 to 131.204.21.179. Redistribution subject to AVS license or copyright; see http://avspublications.org/jvstb/about/rights_and_permissions

generated (when a circuit pattern contains N_c points to be exposed). In this paper, a method which generates only N_p PSF's where $N_p < N_c$ and selects a PSF randomly for each point exposed for calculation of the exposure distribution is described (to be referred to as SMC method). The validity of the method is evaluated through an extensive simulation.

The set of PSF's generated is denoted by $\tilde{S} = \{psf_j | j = 1, \cdots, N_p\}$. In the SMC method, a PSF is randomly selected from the set $\tilde{S}$ for each of N_c points exposed. That is, calculation of the exposure distribution $e(x, y, z)$ can be expressed as (also refer to Fig. 2)

$$e(x,y,z) = \int\int d(x - x', y - y', 0) psf_j(x', y', z)\,dx'dy'. \quad (3)$$

In the above convolution, $j = random(i)$ which returns a random number j given i where $1 \leq i \leq N_c$ and $1 \leq j \leq N_p$. Note that i is the index for points exposed and j is the PSF index. That is, the function $random(\ )$ randomly selects a PSF from $\tilde{S}$ for each point i exposed. In the DMC method, each PSF is used only once for a point exposed in the exposure calculation [Eq. (1)]. But, in the SMC method, it is possible that a PSF is selected for more than one point exposed, i.e., on the average $\frac{N_c}{N_p}$ times.

The two commonly employed measures of the LER are the standard deviation and power spectral density of edge locations. In this study, the standard deviation (σ) and power spectral density ($P(\omega)$) of $e(x, y, z)$ are considered in order to evaluate the validity of the proposed SMC method. The method relies on the fact that the two measures converge as N_p increases. On a layer of resist, σ and $P(\omega)$ are computed along paths parallel to the edge of feature according to Eq. (3). Let $\sigma^{(N_p)}$ and $P^{(N_p)}(\omega)$ denote σ and $P(\omega)$ obtained using N_p PSF's, i.e., $\tilde{S} = \{psf_j | j = 1, \cdots, N_p\}$, respectively. Let us define the "convergence errors" of σ and $P(\omega)$ as follows:

$$\varepsilon_\sigma = \left|\sigma^{(N_c)} - \sigma^{(N_p)}\right|, \quad (4)$$

$$\varepsilon_{P(\omega)} = \left|P^{(N_c)}(\omega) - P^{(N_p)}(\omega)\right|. \quad (5)$$

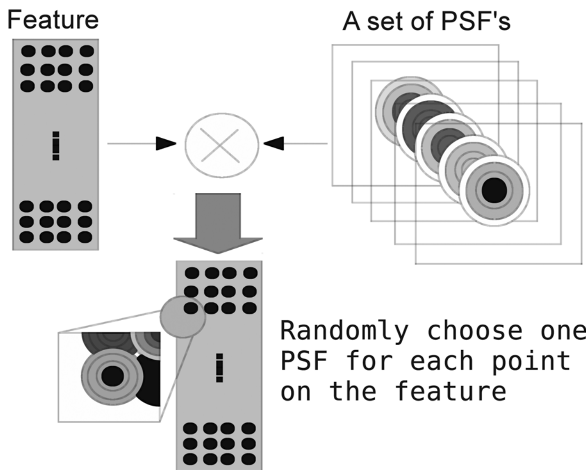

Fig. 2. In the proposed SMC method, a set of PSF's (i.e., instances of stochastic PSF) are generated through the Monte Carlo simulation and the exposure is computed by selecting a PSF randomly from the set for each point exposed during the convolution.

One of the objectives of this study is to find the minimum N_p (denoted by $N_p^{\min}$) which satisfies

$$\lim_{N_p \to N_p^{min}} \varepsilon_\sigma < \epsilon_\sigma, \quad (6)$$

$$\lim_{N_p \to N_p^{min}} \varepsilon_{P(\omega)} < \epsilon_{P(\omega)}, \quad (7)$$

where the thresholds ϵ_σ and $\epsilon_{P(\omega)}$ are small enough that $\sigma^{(N_p^{min})}$ and $P^{(N_p^{min})}(\omega)$ can be considered statistically equivalent to $\sigma^{(N_c)}$ and $P^{(N_c)}(\omega)$, respectively.

The computational complexity of the SMC method is $N_d N_p^{min}$ compared to $N_d N_c$ of the DMC method. In order for the SMC method to be practical, N_p^{min} needs to be much smaller than N_c. Hence, it is necessary to analyze the behaviors of the two measures as functions of N_p. The *reduction factor*, which quantifies the reduction in the computational requirement (for generating PSF's) by the SMC method over the DMC method, is defined as the ratio of the computational complexity of the DMC method to that of the SMC method. That is,

$$\text{reduction factor} = \frac{N_d N_c}{N_d N_p^{min}} = \frac{N_c}{N_p^{min}}. \quad (8)$$

Note that the larger the reduction factor is, the greater the computational saving by the SMC method is.

V. EVALUATION

The validity of the SMC method has been examined through an extensive simulation with single-feature and multifeature patterns.

A. Model and measures

The resist layer in the substrate system in Fig. 1 may be considered as a stack of thin resist layers as shown in Fig. 3. It is assumed that a feature of size $W \times L$ (or features) is long in the Y-dimension (see Fig. 4). The Z-axis is along the resist depth dimension. Given a feature (or features) exposed, the 3D exposure distribution is computed layer-by-layer through convolution between the dose distribution function and the 3D point spread function. Based on the exposure distribution

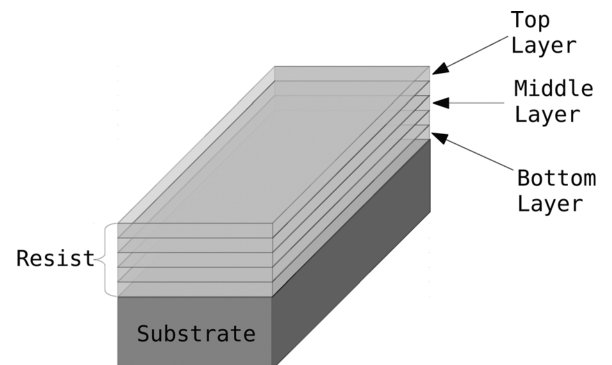

Fig. 3. Resist system is modeled by multiple thin layers. In this study, the top, middle, and bottom layers are considered.

Downloaded 10 Dec 2012 to 131.204.21.179. Redistribution subject to AVS license or copyright; see http://avspublications.org/jvstb/about/rights_and_permissions

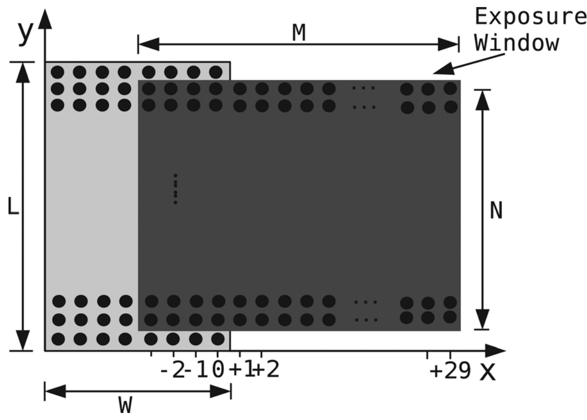

FIG. 4. In the simulation study, the exposure is computed within an exposure window in each layer, which is partially overlapped with a feature so that the exposure fluctuation is analyzed in both exposed and unexposed regions.

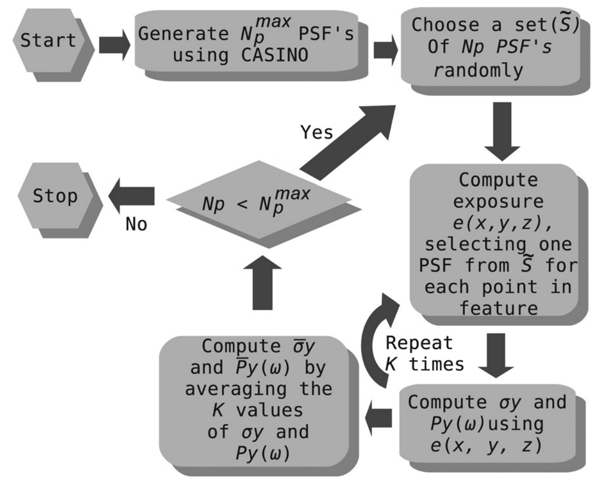

FIG. 5. Flowchart of SMC simulation.

computed within the *exposure window* of size $M \times N$ (see Fig. 4) in each layer, the two measures of exposure fluctuation are derived, i.e., standard deviation (σ) and power spectral density ($P(\omega)$).

Given X (the distance from the feature edge) and Z (resist layer), the standard deviation of exposure distribution (along a line parallel to the Y-axis: refer to Fig. 4) is computed by

$$\sigma_y = \sqrt{\frac{1}{N}\sum_y (e(X,y,Z) - \bar{e}_y(X,Z))^2}, \tag{9}$$

where $\bar{e}_y(X,Z) = \frac{1}{N}\sum_y e(X,y,Z)$.

Similarly, given X and Z, the power spectral density is computed as

$$P_y(\omega) = |F_y(\omega)|^2, \tag{10}$$

where $F_y(\omega)$ is the discrete Fourier transform of exposure distribution, i.e., $\frac{1}{N}\sum_y e(X,y,Z)e^{-j\omega y}$ and therefore the discrete frequency ω ranges from 0 to $\omega_{max} = \frac{N}{2}$.

B. Procedures

The procedures for evaluating the SMC method by computing the two measures, SD (σ_y) and PSD ($P_y(\omega)$), with N_p varied are depicted below (also refer to the flowchart in Fig. 5):

Step 1: Generate N_p^{max} (stochastic) PSF's where $N_p^{max} < N_c$. Initialize N_p to a small value, e.g., 1.
Step 2: Choose N_p PSF's randomly to get $\tilde{S} = \{psf_j | j = 1, \cdots, N_p\}$.
Step 3: Compute the layer-by-layer three-dimensional exposure $e(x, y, z)$ within the exposure window, randomly selecting a PSF from $\tilde{S}$ for each point in the feature exposed.
Step 4: Compute σ_y and $P_y(\omega)$ using $e(x, y, z)$ obtained in Step 3.
Step 5: Repeat Steps 3 and 4 K times using the same N_p PSF's (note that the PSF for a point in the feature is randomly selected). Compute $\bar{\sigma}_y$ and $\bar{P}_y(\omega)$ by averaging the K values (samples) of σ_y and $P_y(\omega)$, respectively.
Step 6: Increase N_p. Go back to Step 2 if $N_p < N_p^{max}$.

The reason for computing $\bar{\sigma}_y$ and $\bar{P}_y(\omega)$ in Step 5, i.e., the average σ_y and $P_y(\omega)$, is to obtain more statistically stable results.

C. Single feature

A long rectangular feature is employed in order to analyze the behaviors of SD and PSD of $e(x, y, z)$ computed by the SMC method as functions of N_p where N_p^{max} is much smaller than N_c. As shown in Fig. 4, an exposure window is partially overlapped with the feature so that the fluctuation of exposure inside and outside the feature can be examined.

For a realistic size of feature, generating N_c PSF's would take a very long time. In order to test the SMC method for the case where $N_p^{max} = N_c$ for completeness, a small size of rectangular feature is also considered. Since we reduce the feature size, the size of exposure window is reduced correspondingly.

D. Multiple features

The SMC method is also tested for a pattern of multiple features. A pattern of multiple lines shown in Fig. 6 is employed in order to examine the dependency of the behaviors of SD and PSD on location in a pattern. The two locations, corner and center, within the pattern are considered and the fluctuation of exposure inside and outside the feature is observed. In a multifeature pattern, the exposure level varies with location in the pattern even when the same features are uniformly distributed. Accordingly, the absolute values of the measures (SD and PSD) also depend on location. In order to compare the statistical behaviors of the measures at the corner and center locations excluding the effect of the spatially varying exposure level, the measures are normalized: the SD by the sum of SD's within the exposure window, and each frequency component (of PSD) by the sum of all frequency components given a column within the exposure window. Note that both sums are proportional to the exposure level,

$$\hat{\sigma}_y = \frac{\bar{\sigma}_y(X)}{\sum_{i=1}^{M}\bar{\sigma}_y(X=i)}, \tag{11}$$

Downloaded 10 Dec 2012 to 131.204.21.179. Redistribution subject to AVS license or copyright; see http://avspublications.org/jvstb/about/rights_and_permissions

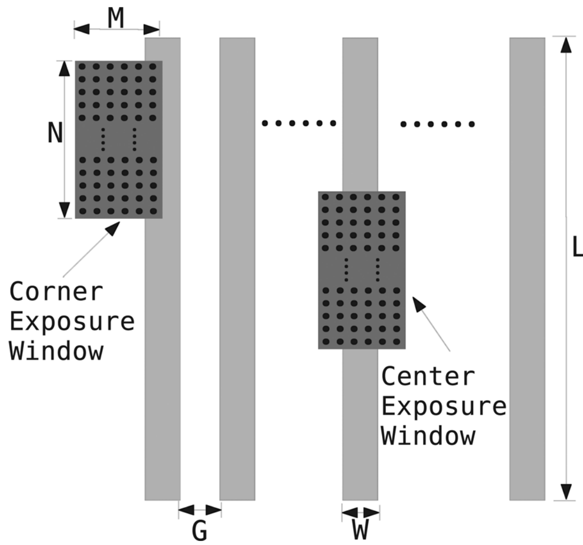

FIG. 6. Expected dependency of exposure fluctuation on location in a large pattern is verified with the exposure window placed in the corner and center regions.

$$\hat{P}_y(\omega) = \frac{\bar{P}_y(\omega)}{\sum_{i=0}^{\omega^{max}} \bar{P}_y(\omega = i)}, \tag{12}$$

where M is the width of exposure window and ω^{max} is the highest frequency in the PSD (refer to Sec. V A).

VI. RESULTS AND DISCUSSION

The CASINO software[14] is employed to generate stochastic PSF's. In the substrate system employed, a 300 nm layer of PMMA (poly(methyl methacrylate)) is on top of Si. The beam energy is set to 50 keV with the beam diameter of 3 nm. Each feature is exposed with the uniform dose of 640 $\mu C/cm^2$ and the unit of exposure is eV/nm^3. The resist PMMA is modeled by five layers and the top, middle, and bottom layers are analyzed in this study.

In the simulation study, three test cases are considered in terms of pattern, i.e., a single long rectangle, a single small rectangle, and multiple long lines. The size of the long rectangular feature is $8 \times 300\,(W \times L)$, i.e., $N_c = 2400$, with which the exposure window of $32 \times 256\,(M \times N)$ is overlapped where the pixel size (interval) is 5 nm. The size of the small rectangular feature is 4×50, i.e., $N_c = 200$, and that of the corresponding exposure window is 32×32. In the multiline pattern, there are 11 lines where the size of each line is 8×368, i.e., $N_c = 32384$, and the space between lines is 8. The exposure window of 9×32 is placed at the corner and center of the pattern. The domain of PSF is 400×400.

The exposure distributions right outside the edge ($X=1$) of the long rectangular feature are shown in Fig. 7. It is seen that there exists a significant difference in the exposure level among the resist layers. Also, the degree of exposure fluctuation varies with resist layer. In Figs. 8 and 9, $\bar{\sigma}_y$ for $X=0$ and 1 and $\bar{P}_y(\omega)$ for $X=0$ are plotted as functions of N_p. As N_p increases, both of $\bar{\sigma}_y$ and $\bar{P}_y(\omega)$ initially vary significantly, but eventually converge. It can be seen that the value of N_p for which $\bar{\sigma}_y$ and $\bar{P}_y(\omega)$ converge is well below 100, i.e., $N_p^{min} < 100$, much smaller than $N_c = 2400$. That is, the reduction factor [refer to Eq. (8)] is greater than 24. In more detail, $\bar{\sigma}_y$ converges fastest in the top layer and slowest in

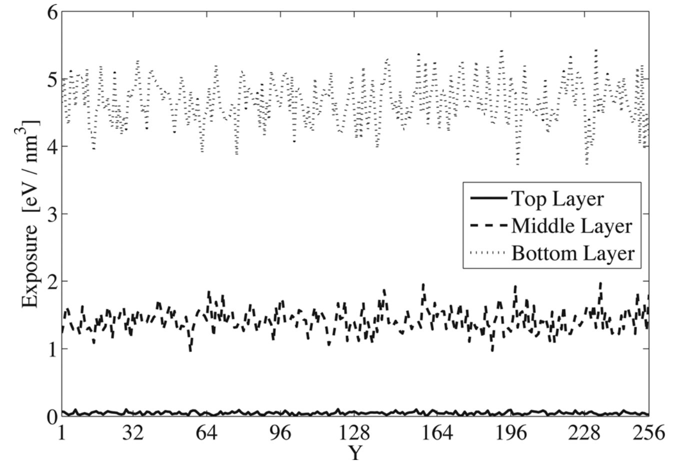

FIG. 7. Exposure level and fluctuation vary with resist layer.

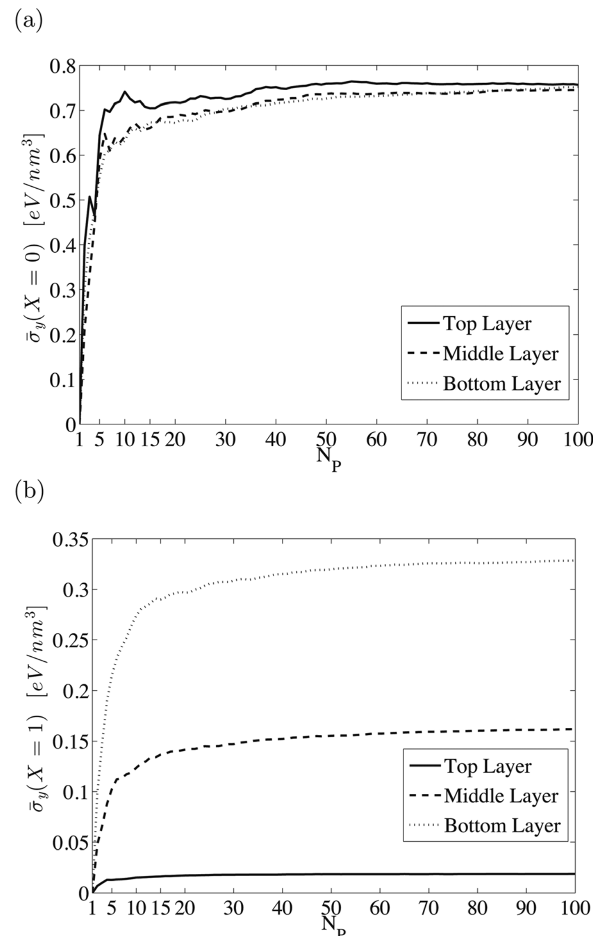

FIG. 8. Average standard deviation ($\bar{\sigma}_y$) obtained from the long rectangular feature where $N_c = 2400$ (refer to Sec. V B). The average exposure for $X=0$ is 15.40, 15.41, and 15.36 for the top, middle, and bottom layers, respectively, and the average exposure for $X=1$ is 0.03, 1.08, and 3.47 for the top, middle, and bottom layers, respectively.

Downloaded 10 Dec 2012 to 131.204.21.179. Redistribution subject to AVS license or copyright; see http://avspublications.org/jvstb/about/rights_and_permissions

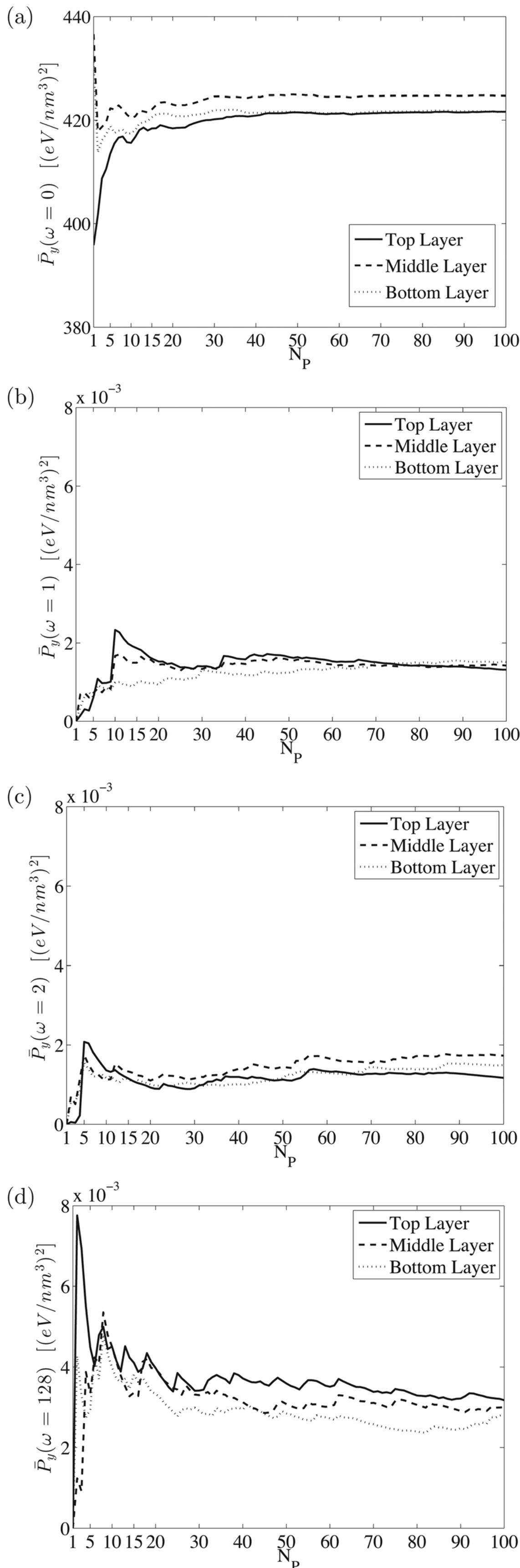

FIG. 9. Average power spectral density ($\bar{P}_y(\omega)$) obtained from the long rectangular feature where $N_c = 2400$ (refer to Sec. V B). The average exposure for $X = 0$ is 15.40, 15.41, and 15.36 for the top, middle, and bottom layers, respectively.

the bottom layer (see Fig. 8). The lower frequency component of $\bar{P}_y(\omega)$ tends to converge faster (see Fig. 9). A higher frequency component would require averaging over more PSF's before it converges to a stable value, canceling out the statistical fluctuation.

The small rectangular feature is employed to check for the completeness of results, i.e., to see if there is any change in the behaviors of SD and PSD beyond the convergence. N_p is varied from 1 to N_c which is 200 (4×50). The behaviors of SD and PSF are analyzed in terms of their percent convergence errors defined as follows:

$$\eta_\sigma = \frac{\varepsilon_\sigma}{\sigma^{(N_c)}} \times 100\%, \tag{13}$$

$$\eta_{P(\omega)} = \frac{\varepsilon_{P(\omega)}}{P^{(N_c)}(\omega)} \times 100\%. \tag{14}$$

In Table I, η_σ is provided for $X = 2$. It can be seen that the convergence error monotonically decreases as N_p increases from 1 to N_c, which demonstrates the accuracy of SMC method. Therefore, one can stop increasing N_p once the convergence error reaches an acceptable value. For example, $N_p = 80$ in this case when the acceptable convergence error is 5%.

In Figs. 10 and 11, $\hat{\sigma}_y$ for $X = 0$ and 1 and $\hat{P}_y(\omega)$ for $X = 0$ obtained for the multiline pattern are provided. The similar convergence behaviors of SD and PSD can be observed where N_p^{min} is below 200 (so the reduction factor is at least 160). As expected, both of $\hat{\sigma}_y$ and $\hat{P}_y(\omega)$ are larger in the corner region than in the center region. Note that the exposure in the center region is statistically more stable, i.e., a smaller fluctuation since more exposed points contribute exposure to the points in the center region, i.e., more averaging is carried out, compared to the corner region. Due to the same reason, there is a smaller difference in both measures among the three layers in the center region.

Based on the above analysis, it can be said that the SMC method generates simulation results statistically equivalent to those by the DMC method with small errors in terms of the two measures, SD and PSD, and the reduction in the computational requirement is larger for a larger pattern.

VII. SUMMARY

A computer simulation is often employed in many lithography research and development efforts. In order for the simulation to be practical, it must be not only accurate but also fast. In e-beam lithography, the stochastic fluctuation of

TABLE I. Percent convergence error of SD as a function of the number of PSF's used (N_p), obtained from the small regular feature where $N_c = 200$.

	Number of PSF's used (N_p)								
Layer	5	10	20	40	60	80	100	140	180
Top	41.71	31.29	27.44	13.34	6.45	4.26	3.00	1.65	0.41
Middle	32.97	24.37	10.29	4.55	3.75	1.56	0.68	0.98	0.24
Bottom	39.76	22.50	12.25	6.26	4.57	3.56	2.46	0.44	0.01

Downloaded 10 Dec 2012 to 131.204.21.179. Redistribution subject to AVS license or copyright; see http://avspublications.org/jvstb/about/rights_and_permissions

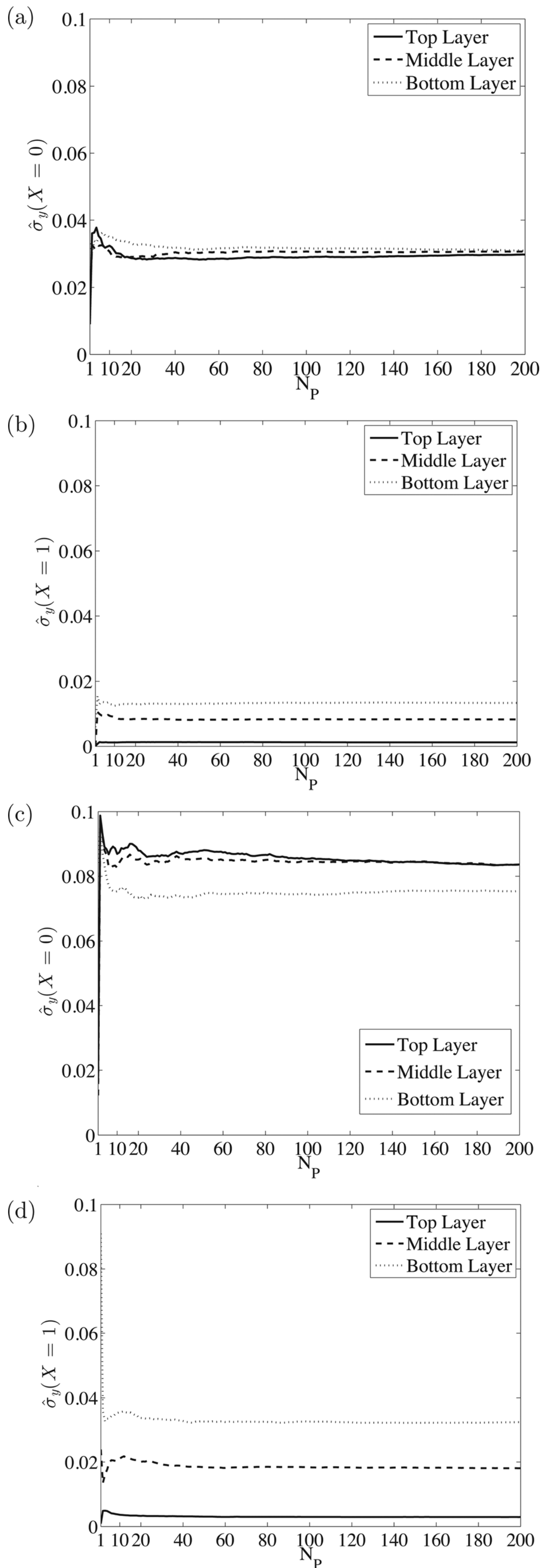

FIG. 10. Normalized standard deviation ($\hat{\sigma}_y$) from the multiline pattern where $N_c = 32384$, in the center region: (a) and (b), and the corner region: (c) and (d). Note that $\hat{\sigma}_y$ is unitless (refer to Sec. V D).

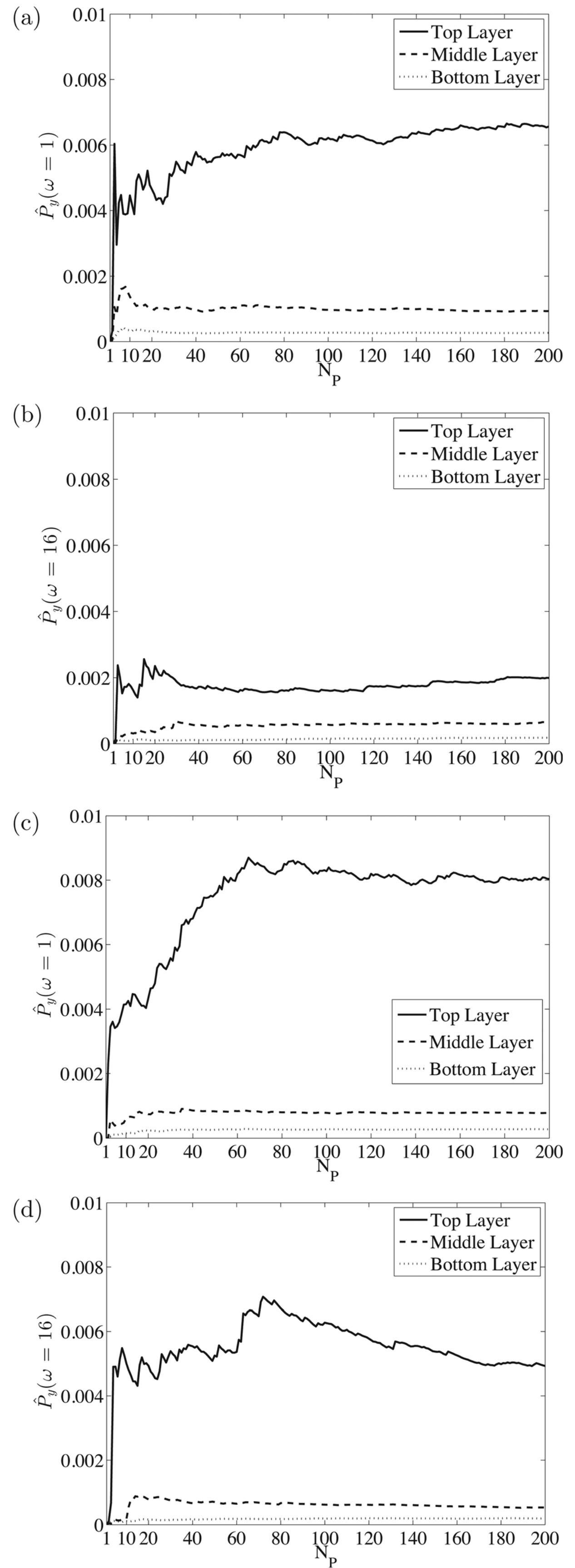

FIG. 11. Normalized power spectral density ($\hat{P}_y(\omega)$: refer to Sec. V D) obtained from the multiline pattern where $N_c = 32384$, in the center region: (a) and (b), and the corner region: (c) and (d). Note that $\hat{P}_y(\omega)$ is unitless (refer to Sec. V D).

Downloaded 10 Dec 2012 to 131.204.21.179. Redistribution subject to AVS license or copyright; see http://avspublications.org/jvstb/about/rights_and_permissions

exposure in the resit is one of the main factors contributing to the LER. A direct method to simulate the exposure fluctuation is to carry out the Monte Carlo simulation at every point exposed. While this method can provide realistic results, it can be too time-consuming to be employed in practice. In this paper, a new method which can cut down the required computation by orders of magnitude and still produce the simulation results statistically equivalent to those by the direct method with an acceptable error is described. It is based on the fact that one is interested in certain measures of the exposure fluctuation, not the exact distribution of exposure itself. It generates a relatively small number of PSF's and chooses a PSF randomly for each point exposed. The new method is simple, but it provides us with an effective tool for simulation of the stochastic exposure distribution. With the two measures of standard deviation and power spectral density in quantifying the exposure fluctuation, the validity of the new method has been evaluated through computer simulation. The current study includes the theoretical verification of the simulation results in this paper.

ACKNOWLEDGMENT

This work was supported by a research grant from Samsung Electronics, Co., Ltd.

[1]R. Murali, D. Brown, K. Martin, and J. Meindl, J. Vac. Sci. Technol. B **24**, 2936 (2006).
[2]F. Hu and S.-Y. Lee, J. Vac. Sci. Technol. B **21**, 2672 (2003).
[3]Q. Dai, S.-Y. Lee, S.-H. Lee, B.-G. Kim, and H.-K. Cho, J. Vac. Sci. Technol. B **29**, 06F314 (2011).
[4]Q. Dai, S.-Y. Lee, S.-H. Lee, B.-G. Kim, and H.-K. Cho, Microelectron. Eng. **88**, 902 (2011).
[5]H. Eisenmann, T. Waas, and H. Hartmann, J. Vac. Sci. Technol. B **11**, 2741 (1993).
[6]S.-Y. Lee and B. D. Cook, IEEE Trans. Semicond. Manuf. **11**, 117 (1998).
[7]M. Osawa, K. Takahashi, M. Sato, and H. Arimoto, J. Vac. Sci. Technol. B **19**, 2483 (2001).
[8]M. Nagase, H. Namatsu, K. Kurihara, K. Iwadate, K. Murase, and T. Makino, Jpn. J. Appl. Phys., Part 1 **35**, 4166 (1996).
[9]C. M. Nelson, S. C. Palmateer, and T. Lyszczarz, Jpn. J. Appl. Phys., Part 1 **38**, 7114 (1999).
[10]M. Evaldsson, I. V. Zozoulenko, H. Xu, and T. Heinzel, Phys. Rev. B **78**, 161407 (2008).
[11]T. C. Li and S. P. Lu, Phys. Rev. B **77**, 85408 (2008).
[12]G. Fiori and G. Iannaccone, IEEE Electron Device Lett. **28**, 760 (2007).
[13]S. Johnson, "Simulation of electron scattering in complex nanostructures: Lithography, metrology, and characterization," Ph.D. dissertation (Cornell University, Ithaca, New York, 1992).
[14]D. Drouin, A. R. Couture, D. Joly, X. Tastet, V. Aimez, and R. Gauvin, Scanning **29**, 1 (2007).
[15]S.-Y. Lee, Q. Dai, S.-H. Lee, B.-G. Kim, and H.-K. Cho, J. Vac. Sci. Technol. B **29**, 06F902 (2011).
[16]J. Zhou and X. Yang, J. Vac. Sci. Technol. B **24**, 1202 (2006).
[17]Q. Dai, S.-Y. Lee, S.-H. Lee, B.-G. Kim, and H.-K. Cho, Microelectron. Eng. **88**, 3054 (2011).
[18]R. A. Lawson and C. L. Hendersona, J. Vac. Sci. Technol. B **28**, C6S12 (2010).
[19]S. Sardo, F. Giaconmetti, S. Doneda, and U. Colombo, Microelectron. Eng. **85**, 1210 (2008).
[20]M. Hane, T. Ikezawa, and T. Ezaki, *IEEE International Conference on SISPAD*, Boston MA, 3–5 September, 2003, p. 99.

Downloaded 10 Dec 2012 to 131.204.21.179. Redistribution subject to AVS license or copyright; see http://avspublications.org/jvstb/about/rights_and_permissions